2017 American Control Conference
Sheraton Seattle Hotel
May 24–26, 2017, Seattle, USA

Multi-channel physics-based modeling and experimental validation of an uncoated gasoline particulate filter in clean operating conditions

Gabriele Pozzato, Mark A. Hoffman, and Simona Onori*, *Senior Member, IEEE*

***Abstract*— This paper presents the development of a two-dimensional (2-D), multi-channel, Gasoline Particulate Filter (GPF) system model. The GPF is an aftertreatment device designed to reduce soot particulate emissions in gasoline direct injection engines. A first-principle modeling approach using mass, energy and momentum balance equations is used to describe the clean filter dynamics. The 2D model is simulated by finite element analysis and the unknown model parameters are identified using a Particle Swarm Optimization (PSO) algorithm over experimental data from a GPF instrumented with 15 thermocouples. A validation study is presented that shows the effectiveness of the model proposed. The novel 2D GPF dynamics constitute the modeling foundation needed for the development of control-oriented models that will be explored in future works.**

NOMENCLATURE

$T = T(x,y,t)$ simulated temperature $[K]$
$\mathbf{u} = \mathbf{u}(x,y,t)$ exhaust gas velocity field $\left[\frac{m}{s}\right]$
$\mathbf{v} = \mathbf{v}(x,y,t)$ exhaust gas Darcy velocity field $\left[\frac{m}{s}\right]$
$p = p(x,y,t)$ exhaust gas pressure $[Pa]$
$k = k(x,y,t)$ exhaust gas thermal conductivity $\left[\frac{W}{m\ K}\right]$
$C_p = C_p(x,y,t)$ exhaust gas specific heat capacity at constant pressure $\left[\frac{J}{kg\ K}\right]$
$\rho = \rho(x,y,t)$ exhaust gas density $\left[\frac{kg}{m^3}\right]$
$\mu = \mu(x,y,t)$ exhaust gas dynamic viscosity $[Pa\ s]$
$[c_i] = [c_i](x,y,t)$ $i-th$ species concentration $\left[\frac{mol}{m^3}\right]$
$D_i = D_i(x,y,t)$ $i-th$ species diffusion coefficient $\left[\frac{m^2}{s}\right]$
$\mathcal{T}$ measured temperature $[K]$
v_{inlet} inlet exhaust gas velocity $\left[\frac{m}{s}\right]$
v_{sound} speed of sound at 300 $[K]$, 347 $\left[\frac{m}{s}\right]$ [1]
A_{cross} cross sectional area $[m^2]$
D_H hydraulic diameter $[m]$
V gas volume $[m^3]$
M molar mass $\left[\frac{kg}{mol}\right]$
m mass $[kg]$
$\dot{m}$ mass air flow $\left[\frac{kg}{s}\right]$
θ volumetric flow rate $\left[\frac{m^3}{s}\right]$
X volume fraction $[-]$
n_{tot} combustion kinetics moles of products $[mol]$
R universal gas constant, 8.31 $\left[\frac{J}{mol\ K}\right]$
k_w wall thermal conductivity 1 $\left[\frac{W}{m\ K}\right]$
C_w wall specific heat capacity $\left[\frac{J}{kg\ K}\right]$
ρ_w wall density, 2500 $\left[\frac{kg}{m^3}\right]$
ε_P^w wall porosity, 0.65 $[-]$
κ_w wall permeability, 2.82×10^{12} $[m^2]$
τ_w wall tortuosity $[-]$
ρ_{plug} plug density, 1250 $\left[\frac{kg}{m^3}\right]$
k_{plug} plug conductivity, 0.5 $\left[\frac{W}{m\ K}\right]$
h_{ext} external convective heat transfer coefficient $\left[\frac{W}{m^2\ K}\right]$
T_{ext} room temperature, 300 $[K]$
eff effective property
$inlet/outlet$ inlet/outlet boundaries
$fluid/solid$ porous medium fluid/solid phases
$[\mathcal{X}]$ concentration of a generic species $\mathcal{X}$

Department of Automotive Engineering, International Center for Automotive Research, Clemson University, Greenville, South Carolina 29607
{gpozzat,mhoffm4,sonori}@clemson.edu
* corresponding author

I. INTRODUCTION

Gasoline Direct-Injection (GDI) engine technology improves vehicle fuel economy toward future targets while, simultaneously decreases CO_2 emissions. The main drawback of this efficiency improving technology is the increased emission of particulates (when compared to their indirect injection-based technology counterpart [2]). In general, fuel combustion leads to the production of different air pollutants, among which the most dangerous are HC, CO, NO_x and particulate matter. The Three Way Catalyst (TWC) is a well known solution for reduction of the dangerous gaseous emissions. Indeed, different studies can be found in literature for TWC [3], [4]. Gasoline Particulate Filters (GPF) are considered the aftertreatment technology of choice in order to meet future Particulate Number (PN) targets of $6 \times 10^{11}[\sharp/km]$ [5] imposed by EU6 for GDI engines. A typical strategy for removal of particulates involves the installation of a GPF downstream of the TWC. Similar to the Diesel Particulate Filter (DPF), this device is composed of inlet and outlet channels divided by porous walls made up of Cordierite. The particulate filter traps soot particles (primarily composed of carbon) resulting from fuel combustion, and prevents their release into the atmosphere. Soot oxidation is required at regular intervals to clean the filter, maintaining a consistent soot trapping efficiency, managing the increase in backpressure due to soot accumulation in the filter, and avoiding the formation of soot plugs in the GPF channel. This procedure is known as GPF regeneration [6]. Particulate emission control in gasoline engines is a recently identified challenge, and very little progress has been made to model GPF thermal dynamics. Design optimization of a GPF has been investigated with respect to pressure drop and PN filtration efficiency by Shimoda et al. [7] and Ito et al. [5]. In the work by Nicolin et al. [8] and Boger et al. [9], a reduced order model for thermal dynamics was presented. To properly

Property	
Material	Cordierite
Diameter× Length	$D \times L = 118 \times 127$ $[mm]$
Trapping volume	$V_{trap} = 0.725$ $[l]$
Cell density	300 $[cpsi]$
Cell area	$A = 2.15 \times 10^{-6}$ $[m^2]$
Wall thickness	$h_w = 8.5$ $[mil] = 0.22$ $[mm]$
Channel height	$h_c = 1.03$ $[mm]$
Plug length	$l_p = 7$ $[mm]$

TABLE I: Geometric specifications of the high porosity GPF 300/8

characterize the filter, the authors focus on soot oxidation kinetics by studying the regeneration events inside the filter. Finally, a 1D+1D single-channel model is described by Opitz et al. [10]. In this work, an experimental and simulation study is performed to understand the cold start behaviour of the particulate filter and a comparison with respect to a 2D single-channel *COMSOL Multiphysics®* model is proposed.

Conversely, the DPF utilization is widespread, and a substantial quantity of modeling work has been published. The control oriented model developed by Konstandopoulos[1] [6] captures the thermal behaviour with an ordinary differential equation (ODE). The model does not consider spatial coordinates since it is based on homogeneous assumptions. Alternatively, Koltsakis et al. [12] utilize a 1D model based on partial differential equations (PDEs) to describe transport phenomena in the filter. Opris et al. [13] propose a 2D, physics-based model combining flow and thermal equations.

Improvement in the aftertreatment design has significantly increased the complexity of its composition and dynamic behavior. Advanced control algorithms for the next generation of emission and exhaust gas aftertreatment devices will require discrete spatial knowledge of internal filter temperatures during specific events within the regeneration and soot accumulation. This information will enable control engineers to design more accurate algorithms to optimize and control the soot oxidation events, thus reducing emissions and fuel consumption. In addition, the adoption of advanced development tools such as Software-in-the-Loop (SIL) and Hardware-in-the-Loop (HIL) will be facilitated thanks to properly designed control-oriented models. Significantly reducing the development time and costs associated with emission reduction control system design and calibration.

This paper proposes a 2D physics-based model for uncoated GPF dynamics, its *COMSOL Multiphysics®* implementation and its validation with experimental data. Great emphasis is placed on the thermal dynamics for clean filter operating conditions. Modeling the thermal gradient inside the filter is necessary in order to understand and prevent the formation of cracks or device failures. Future work will discuss regeneration modeling and other GPF issues. The model equations are first described into detail. Then, an identification procedure of the *COMSOL Multiphysics®* model, based on Particle Swarm Optimization (PSO), is presented. Finally, a detailed comparison between the 2D model and experimental data is presented to quantify the model predictiveness during clean filter operating conditions. To the best of the authors' knowledge, such a model constitutes the very first step to build physically-motivated control-oriented models to use for optimization-based control of particulate for new generation engines.

[1]The reader can refer to [11] for detailed discussions on differences between GPF and DPF.

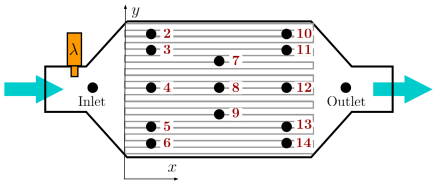

Fig. 1: GPF temperature sensor layout: 15 thermocouples ($\mathcal{T}_{inlet}, \mathcal{T}_{outlet}, \mathcal{T}_i$ with $i = 2, \ldots, 14$) have been used to instrument the uncoated filter tested in this work

II. THE GASOLINE PARTICULATE FILTER

Filter media and geometric configuration have a key role in the GPF system. The selection process for the filter media and geometric configuration depends on different aspects: pressure drop performance, particulate collection efficiency, regeneration, durability and cost. Different geometric configurations and technologies have been studied for DPF but the honeycomb wall-flow monolith design, introduced in 1981 [14], remains the most popular configuration [6]. Thanks to its compact arrangement and filtration efficiency, this geometry is adopted also for the GPF. Different materials can be used as filter media for the active filtration of soot. In our analysis the monolith is made up by Cordierite, a widely used ceramic material. The structural and geometric properties of the GPF used in this work are summarized in Table I. For the purpose of this study, the uncoated filter was instrumented with 15 thermocouples placed according to the layout in Figure 1. The amount of oxygen going into the filter is measured with a wide-band λ sensor.

III. 2D PHYSICS BASED MODEL

A physics based GPF model has been developed in *COMSOL Multiphysics®* for this work. This software predicts phenomena using a finite element approach and solving the physics PDEs. Specifically, the presented model aims to predict the GPF thermal dynamics in both the axial x and y directions. Detailed examination of GPF temperature dynamics is mandatory to avoid cracking the ceramic substrate, leading to filter failure. To describe the physics of the GPF, mass, energy, and momentum (Navier-Stokes) balance equations are employed. In the present work, FEA is applied to a 2D GPF section composed of 47 channels. Each single channel is comprised of one inlet and one outlet channel pair closed by plugs, with a filter wall (porous medium) separating them. Except for some filter specifications such as conductivity, density, porosity and permeability, the other parameters are considered time and space varying in order to obtain a model as close as possible to real operating conditions. Inside the channel plugs, mass and momentum transport can be neglected, hence only energy balance is taken into account.

A. Mass balance equation

The concentration of species in the exhaust gas is described by a mass balance equation. For inlet and outlet channels the following can be applied:

$$\frac{\partial[c_i]}{\partial t} = -\mathbf{u}\cdot\nabla[c_i] + \nabla\cdot(D_i\nabla[c_i]) \tag{1}$$

where $\frac{\partial[c_i]}{\partial t}$ corresponds to the accumulation/consumption of species, $\mathbf{u}\cdot\nabla[c_i]$ describes the convective transport due to the velocity field $\mathbf{u} = u_x\mathbf{i} + u_y\mathbf{j}$ and $\nabla\cdot(D_i\nabla[c_i])$ expresses the diffusion of the different gaseous species.

In order to compute the mass balance over the porous medium, the following macroscale equation is needed:

$$\varepsilon_P^w\frac{\partial[c_i]}{\partial t} = -\mathbf{v}\cdot\nabla[c_i] + \nabla\cdot(D_{eff,i}^w\nabla[c_i]) \tag{2}$$

where $\mathbf{v}$ is the Darcy average velocity [15]. $D_{eff,i}^w$ is the effective diffusion coefficient of the exhaust gas passing through the porous medium and can be calculated with the following formula [10], [16]:

$$Wall: \quad D_{eff,i}^w = \frac{\varepsilon_P^w}{\tau_w}D_i \tag{3}$$

where τ is an empirical coefficient called tortuosity [10].

B. Energy balance equation

The energy balance equation describes the thermal behaviour of the filter. For inlet and outlet channels the following formulation is considered:

$$\rho C_p\frac{\partial T}{\partial t} + \rho C_p(\mathbf{u}\cdot\nabla T) = \nabla\cdot(k\nabla T) \tag{4}$$

where $\rho C_p(\mathbf{u}\cdot\nabla T)$ is the convective energy transport and $\nabla\cdot(k\nabla T)$ is the heat conduction term.

The wall is a porous medium composed of two phases: a solid-phase and a fluid-phase. Hence, the following description is adopted [15].

$$\begin{aligned}&Solid\ phase:\\ &(1-\varepsilon_P)\rho_w C_w\frac{\partial T_{solid}}{\partial t} = (1-\varepsilon_P)\nabla\cdot(k_w\nabla T_{solid})\\ &Fluid\ phase:\\ &\varepsilon_P\rho C_p\frac{\partial T_{fluid}}{\partial t} + \rho C_p(\mathbf{v}\cdot\nabla T_{fluid}) = \varepsilon_P\nabla\cdot(k\nabla T_{fluid})\end{aligned} \tag{5}$$

Assuming $T_{solid} = T_{fluid} = T$, the following equation is obtained:

$$(\rho C_p)_{eff}^w\frac{\partial T}{\partial t} + \rho C_p(\mathbf{v}\cdot\nabla T) = \nabla\cdot(k_{eff}^w\nabla T) \tag{6}$$

The effective terms for heat capacity, density and conductivity are average properties of the wall defined with respect to the filter porosity:

$$\begin{aligned}(\rho C_p)_{eff}^w &= (1-\varepsilon_P^w)\rho_w C_w + \varepsilon_P^w\rho C_p\\ k_{eff}^w &= (1-\varepsilon_P^w)k_w + \varepsilon_P^w k\end{aligned} \tag{7}$$

Plugs in the inlet and outlet channels are considered as solid materials, in which only the energy balance is modeled. Hence, in these domains the thermal dynamics can be described as follows:

$$\rho_{plug}C_w\frac{\partial T}{\partial t} = \nabla\cdot(k_{plug}\nabla T) \tag{8}$$

with $\nabla\cdot(k_{plug}\nabla T)$ the conductive energy transport inside the plugs.

C. Navier-Stokes equation

Two dimensional partial differential equations for momentum transport are considered in both inlet/outlet channels and porous medium. Assuming exhaust gas to be an incompressible fluid, the Navier-Stokes equation for momentum conservation is then used in the channels:

$$\rho\left(\frac{\partial\mathbf{u}}{\partial t} + \mathbf{u}\cdot\nabla\mathbf{u}\right) = -\nabla p + \mu\nabla^2\mathbf{u} \tag{9}$$

where $\rho\frac{\partial\mathbf{u}}{\partial t}$ and $\rho\mathbf{u}\cdot\nabla\mathbf{u}$ are the inertial forces, $-\nabla p$ is the pressure force and $\mu\nabla^2\mathbf{u}$ is the viscous force. The assumption of incompressible fluid is reasonable since the Mach number is much lower than the common threshold of $0.3\ Ma$ [17] (Section V).

In a similar way, the conservation of momentum throughout the porous medium can be expressed using the macroscale equation proposed by Hsu and Cheng [15] given by:

$$\frac{\rho}{\varepsilon_P^w}\left(\frac{\partial\mathbf{v}}{\partial t} + \frac{\mathbf{v}}{\varepsilon_P^w}\cdot\nabla\mathbf{v}\right) = -\nabla p + \frac{\mu}{\varepsilon_P^w}\nabla^2\mathbf{v} - \frac{\mu}{\kappa_w}\mathbf{v} \tag{10}$$

where $\frac{\mu}{\kappa_w}\mathbf{v}$ is penalizing the flow through porous medium based on the material's permeability. Both Navier-Stokes and Hsu-Cheng equations require the following mass continuity equations:

$$\nabla\cdot\mathbf{u} = 0,\ \nabla\cdot\mathbf{v} = 0 \tag{11}$$

The GPF dynamics are described by the system of equations (1), (2), (4), (6), (9), (10) and (11). Since thermal dynamics are much slower than the relevant fluid dynamics, we can safely solve the momentum balance equation in steady-state conditions. Then, mass and energy balance equations are solved using a time-dependent solver. A sensitivity analysis was performed in order to obtain the minimum rectangular mesh complexity able to describe the GPF dynamics.

IV. BOUNDARY CONDITIONS

The partial differential equations for mass, energy and momentum balance are solved while imposing the boundary conditions shown in Figure 2. Hence, the inlet exhaust gas properties must be defined.

A. Mass balance

Upstream the TWC, the exhaust gas is characterized by the following composition:

$$N_2,\ O_2,\ CO_2,\ H_2O,\ HC,\ NO_x,\ CO \tag{12}$$

Assuming optimal operation of the upstream TWC, the concentrations of HC, NO_x, CO can be considered equal to zero. Under the assumption of ideal gas mixture and

Boundary	Condition	Description
Mass balance		
1	$[c_i] = [c_i](y,t)\|_{x=0}$	Inflow concentration of the $i-th$ species.
2/6	$-\mathbf{n}\cdot\mathbf{N}_i = 0$ $\mathbf{N}_i = -D_i\nabla[c_i] + \mathbf{u}[c_i]$	No mass flow.
3	$-\mathbf{n}\cdot D_i\nabla[c_i] = 0$	The dominating transport in outflow is convection, diffusion is ignored.
Momentum balance		
1	$\mathbf{u} = \mathbf{u}(y,t)\|_{x=0} = u_x^{inlet}\mathbf{i} + u_y^{inlet}\mathbf{j}$	Inlet fluid velocity.
2/6	$\mathbf{u} = \mathbf{0}$	No viscous effects at the slip wall.
3	$p = p_{outlet}$ $[\mu(\nabla\mathbf{u} + (\nabla\mathbf{u})^T)]\mathbf{n} = \mathbf{0}$	No viscous stress in outlet.
Energy balance		
4	$T = T(y,t)\|_{x=0}$	Exhaust gas inlet temperature.
6	$-\mathbf{n}\cdot(k\nabla T) = h_{ext}\ (T_{ext} - T)$	External convective heat exchange.
5	$-\mathbf{n}\cdot(k\nabla T) = 0$	No conduction in outflow.

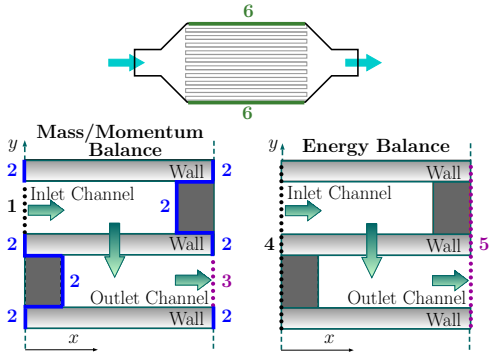

Fig. 2: Table on the left lists the PDE boundary conditions with respect to different channel parts depicted on the right and numbered $1, 2, 3, 4, 5, 6$

considering the GPF measured inlet temperature $\mathcal{T}_{inlet}$, the exhaust gas density can be determined by:

$$\rho_{inlet} = \frac{M_{tot}\ p}{R\ \mathcal{T}_{inlet}(t)} \tag{13}$$

with M_{tot} the total molar mass:

$$M_{tot} = \sum_i X_i\ M_i = X_{N_2}\ M_{N_2} + X_{O_2}\ M_{O_2} + X_{CO_2}\ M_{CO_2} + X_{H_2O}\ M_{H_2O} \tag{14}$$

and X_i represents the volume fractions of the different gaseous species. Since the exhaust gas composition changes with respect to the engine operating conditions, an analysis of the fuel combustion kinetics is necessary. For a clean filter operating in stoichiometric conditions ($\lambda = 1$), the following reaction 15 [18] holds true:

$$C_aH_b + \left(a + \frac{b}{4}\right)(O_2 + 3.773N_2) \rightarrow a\ CO_2 + \frac{b}{2}\ H_2O + 3.773\left(a + \frac{b}{4}\right)\ N_2 \tag{15}$$

Hence, defining the total moles of product:

$$n_{tot} = a + \frac{b}{2} + 3.773\ \left(a + \frac{b}{4}\right) \tag{16}$$

and considering $C_aH_b = C_8H_{18}$ (octane), the volume fractions for the different species can be computed:

$$X_{N_2} = \frac{3.773\ (a + b/4)}{n_{tot}} = 0.74,\ X_{O_2} = \frac{0}{n_{tot}} = 0$$
$$X_{CO_2} = \frac{a}{n_{tot}} = 0.12,\ X_{H_2O} = \frac{b/2}{n_{tot}} = 0.14 \tag{17}$$

The volume fractions remain constant over time if conditions downstream of the TWC remain stoichiometric. Finally, the inlet $i-th$ species concentration can be computed with the following:

$$[c_i](y,t)\big|_{x=0} = \frac{X_i\ \rho_{inlet}}{M_{tot}} \tag{18}$$

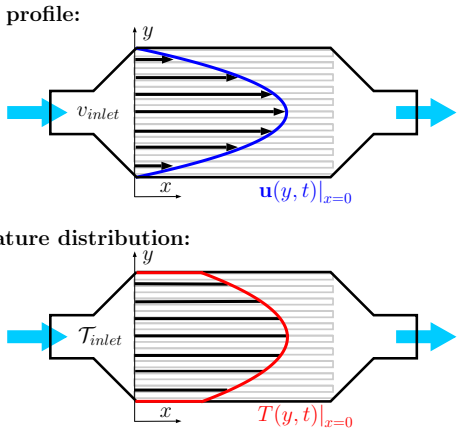

Fig. 3: Exhaust gas velocity profile and temperature distribution

B. Energy balance

Under the assumption of fully developed thermal flow, the following inlet temperature distribution is considered:

$$T(y,t)\big|_{x=0} = \mathcal{B}\ \mathcal{T}_{inlet}(t)\ + (1-\mathcal{B})\ \mathcal{T}_{inlet}(t)\left[1 - \left(\frac{D/2 - y}{D/2}\right)^2\right] \tag{19}$$

where $\mathcal{T}_{inlet}$ is the measured inlet temperature and $\mathcal{B}$ a dimensionless parameter identified in Section V. Equation (19) is the inlet boundary condition for the energy balance equation defined with respect to $x = 0$ (Figure 3).

C. Navier-Stokes equation

Starting from the definitions of mass air flow (MAF) and volumetric flow rate equation (20) is obtained:

$$v_{inlet}(t) = \frac{\dot{m}_{inlet}(t)}{\rho_{inlet}\ A_{cross}^{eff}} \tag{20}$$

where $A_{cross}^{eff} = A_{cross}/2 = \pi(D/2)^2/2$ is the effective cross sectional area taking into account only the open inlet channels. Under the assumption of fully developed flow, a parabolic distribution (Figure 3) is used to describe the inlet

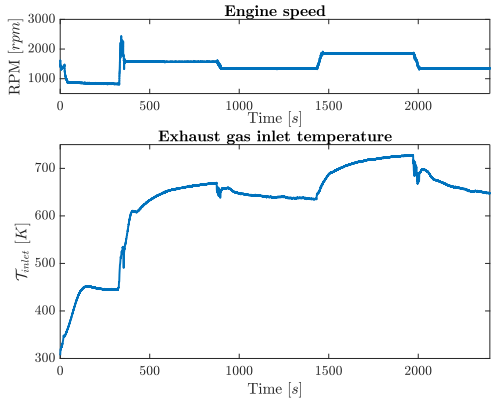

Fig. 4: Engine RPM profile and corresponding measured GPF inlet temperature

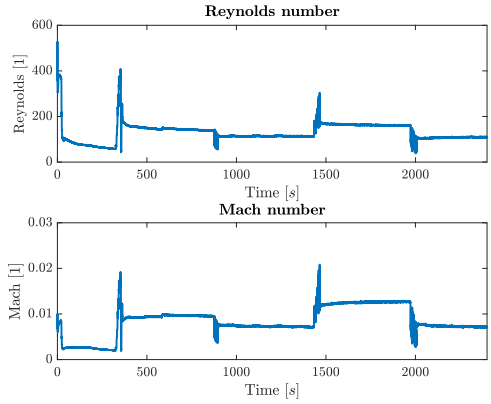

Fig. 5: Reynolds and Mach numbers computed for the maximum speed $\mathcal{A}$ $v_{inlet}(t)$ (for $\mathcal{A} = 2.06$). Reynolds is lower than 2000, hence, a laminar flow regime is assumed [20]. Mach is lower than 0.3, hence, the incompressible Navier-Stokes equations can be applied [17]

exhaust gas velocity profile:

$$\mathbf{u}(y,t)\big|_{x=0} = u_x^{inlet}\mathbf{i} + u_y^{inlet}\mathbf{j}$$
$$\begin{cases} u_x^{inlet} = \mathcal{A}\ v_{inlet}(t)\ \left[1 - \left(\frac{D/2-y}{D/2}\right)^2\right] \\ u_y^{inlet} = 0 \end{cases} \tag{21}$$

where $\mathcal{A}$ is a dimensionless parameter identified in Section V.

V. MODEL IDENTIFICATION

Considering a clean GPF, parameters $\mathcal{A}$ in (21) and $\mathcal{B}$ in (19) together with the external convective heat transfer coefficient h_{ext} are identified using PSO [19] algorithm. Hence, minimizing the following cost function the parameter vector $\theta = [\mathcal{A}, \mathcal{B}, h_{ext}]$ is identified:

$$J(\theta) = \sum_k \sqrt{\frac{1}{N}\sum_i^N (\mathcal{T}_k - T_k(\theta))^2} \tag{22}$$

where N is the number of data samples. In order to best capture both the longitudinal and radial temperature distributions, the optimization problem is solved using sensors $k = \{2, 3, 7, 8, 10\}$ (Figure 1). Results from PSO runs after six days of iterations are shown in Table II. In order to properly identify these parameters, an *ad hoc* experiment is designed and conducted with a vehicle on a chassis dynamometer. By commanding step variations in engine speed (RPM) of ± 250 $[rpm]$ around a mean value of 1600 $[rpm]$ via throttle step changes while the chassis dyno is operated in road-load mode, the desired temperature dynamics, necessary for identification purposes, are obtained. In Figure 4, the RPM profile and the correspondent measured inlet thermal dynamics are shown.

Parameter	Initial guess	PSO search domain	Identified parameter
$\mathcal{A}$ $[-]$	1.72	$[1.63, 2.06]$	2.00
$\mathcal{B}$ $[-]$	0.91	$[0.82, 1.00]$	0.92
h_{ext} $\left[\frac{W}{m^2\ K}\right]$	32.20	$[27.37, 37.03]$	29.51

TABLE II: Parameters identification

As shown in Figure 5, the properties of the fluid are characterized by Reynolds (Re) and Mach (Ma) numbers:

$$Re = \frac{\rho_{inlet}\ v_{inlet}(t)\ D_H}{\mu}, \quad Ma = \frac{v_{inlet}(t)}{v_{sound}} \tag{23}$$

VI. MODEL VALIDATION RESULTS

In this section, a comparison between the bidimensional multi-channel model and experimental results is presented. In order to quantify the model predictability, this validation is performed over a different dataset than that used for identification. The experiment is similar to the one proposed in Section V for model identification, but considers an engine speed variation of ± 150 $[rpm]$ around 1600 $[rpm]$. Performance of the model is accessed by means of the percentage Root Mean Square Error (RMSE), shown on Table III. Figure 6 shows the comparison for thermocouples at the GPF inlet, mid and outlet locations. The performance of the model is characterized by a RMSE lower than 3% (Table III) for all the thermocouple locations. An underpredicting behavior is shown while studying location 14. The reduced accuracy at location 14 is due to asymmetry between locations 10 and 14 in the experimental data. Note that location 10 was utilized during the model identification. Identification of symmetric temperature and velocity profiles can not capture these asymmetries, thus the higher RMSE in location 14.

VII. CONCLUSION

In this paper, a 2D multi-channel GPF model is developed and analyzed for a clean filter operating scenario. Mass, energy and momentum balance equations are used in order to describe the filter thermal dynamics. Identification of unknown model parameters is performed using PSO and a comparative analysis between experimental data and FEA simulation data is shown. The proposed model is able to capture the thermal dynamics at different GPF thermocouple locations, showing a RMSE lower than 2% with the only exception being the identification of thermocouple 14 (2.48%). Hence, the 2D multi-channel model can predict with reasonable error the thermal dynamics of the GPF.

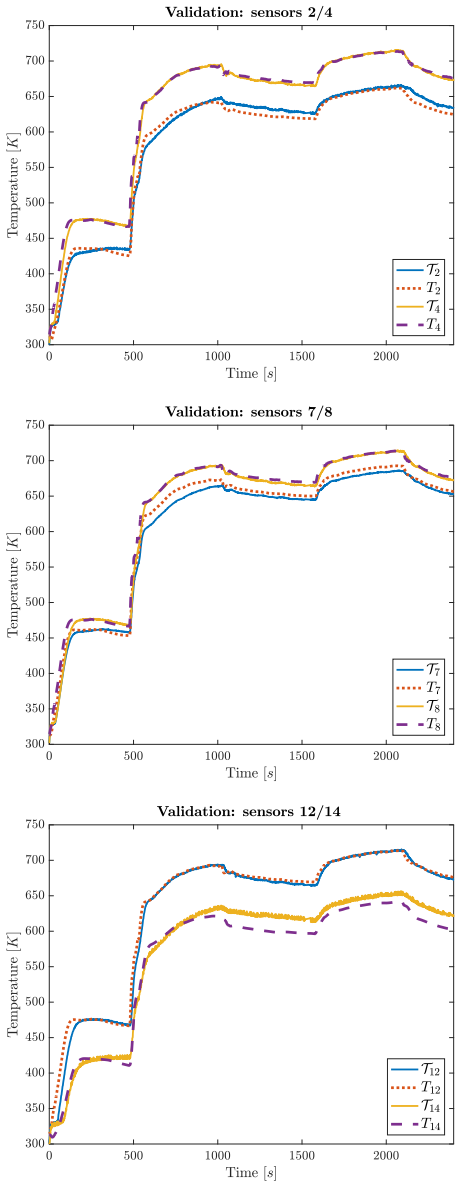

Fig. 6: Validation results of the 2D model against experimental data using Thermocouples in locations $2/4$*,* $7/8$ *and* $12/14$ *are analyzed*

Thermocouple	**Identification RMSE** [%]	**Validation RMSE** [%]
2	1.32	1.35
3	1.20	1.12
4	1.30	1.21
5	1.55	1.56
6	1.77	1.33
7	1.62	1.42
8	1.62	1.48
9	1.39	1.30
10	2.13	1.97
11	1.92	1.97
12	1.85	1.80
13	1.47	1.40
14	2.95	2.48

TABLE III: RMSE calculation for identification and validation datasets. Different sensors locations defined in Figure 1 are considered

Future work will consider filter soot loading and soot burning reactions to model the regeneration event inside the uncoated GPF.

ACKNOWLEDGEMENT

The authors greatly acknowledge the financial support from FCA US LLC (Auburn Hills, MI 48326 USA), under which this work was conducted.

REFERENCES

[1] T. L. Bergman, F. P. Incropera, D. P. DeWitt, and A. S. Lavine, *Fundamentals of heat and mass transfer*. John Wiley & Sons, 2011.

[2] S. Ashley, "Attacking gdi engine particulate emissions, http://articles.sae.org/13624/,"

[3] P. Kiwitz, C. Onder, and L. Guzzella, "Control-oriented modeling of a three-way catalytic converter with observation of the relative oxygen level profile," *Journal of Process Control*, 2012.

[4] T. S. Auckenthaler, C. H. Onder, H. P. Geering, and J. Frauhammer, "Modeling of a three-way catalytic converter with respect to fast transients of λ-sensor relevant exhaust gas components," *Industrial & engineering chemistry research*, 2004.

[5] Y. Ito, T. Shimoda, T. Aoki, K. Yuuki, H. Sakamoto, K. Kato, D. Thier, P. Kattouah, E. Ohara, and C. Vogt, "Next generation of ceramic wall flow gasoline particulate filter with integrated three way catalyst," *SAE Technical Paper 2015-01-1073*, 2013.

[6] A. G. Konstandopoulos, M. Kostoglou, E. Skaperdas, E. Papaioannou, D. Zarvalis, and E. Kladopoulou, "Fundamental studies of diesel particulate filters: transient loading, regeneration and aging," *SAE Technical Paper 2000-01-1016*, 2000.

[7] T. Shimoda, Y. Ito, C. Saito, T. Nakatani, Y. Shibagaki, K. Yuuki, H. Sakamoto, C. Vogt, T. Matsumoto, Y. Furuta, *et al.*, "Potential of a low pressure drop filter concept for direct injection gasoline engines to reduce particulate number emission," *SAE Technical Paper 2012-01-1241*, 2012.

[8] P. Nicolin, D. Rose, F. Kunath, and T. Boger, "Modeling of the soot oxidation in gasoline particulate filters," *SAE Technical Paper 2015-04-14*, 2015.

[9] T. Boger, D. Rose, P. Nicolin, N. Gunasekaran, and T. Glasson, "Oxidation of soot (printex® u) in particulate filters operated on gasoline engines," *Emission Control Science and Technology*, 2015.

[10] B. Opitz, A. Drochner, H. Vogel, and M. Votsmeier, "An experimental and simulation study on the cold start behaviour of particulate filters with wall integrated three way catalyst," *Applied Catalysis B: Environmental*, 2014.

[11] T. W. Chan, E. Meloche, J. Kubsh, D. Rosenblatt, R. Brezny, and G. Rideout, "Evaluation of a gasoline particulate filter to reduce particle emissions from a gasoline direct injection vehicle," *SAE International Journal of Fuels and Lubricants*, vol. 5, no. 2012-01-1727, pp. 1277–1290, 2012.

[12] G. C. Koltsakis and A. M. Stamatelos, "Modes of catalytic regeneration in diesel particulate filters," *Industrial & engineering chemistry research*, 1997.

[13] C. N. Opris and J. H. Johnson, "A 2-d computational model describing the heat transfer, reaction kinetics and regeneration characteristics of a ceramic diesel particulate trap," *SAE Technical Paper 1998-02-980546*, 1998.

[14] J. S. Howitt and M. R. Montierth, "Cellular ceramic diesel particulate filter," *SAE Technical Paper 810114*, 1981.

[15] D. A. Nield and A. Bejan, *Convection in porous media*. Springer Science & Business Media, 2006.

[16] O. Krocher, M. Elsener, and M. Votsmeier, "Determination of effective diffusion coefficients through the walls of coated diesel particulate filters," *Industrial & Engineering Chemistry Research*, 2009.

[17] P. Kundu and L. Cohen, "Fluid mechanics, 638 pp," *Academic, Calif*, 1990.

[18] J. B. Heywood *et al.*, *Internal combustion engine fundamentals*. Mcgraw-hill New York, 1988.

[19] S. Ebbesen, P. Kiwitz, and L. Guzzella, "A generic particle swarm optimization matlab function," in *2012 American Control Conference (ACC)*, IEEE, 2012.

[20] K. Avila, D. Moxey, A. de Lozar, M. Avila, D. Barkley, and B. Hof, "The onset of turbulence in pipe flow," *Science*, 2011.